

Structure and Catalytic Activity of Sb Oxide Highly Dispersed on SnO₂ for Propene Oxidation

TAKEHIKO ONO,¹ TOSHIO YAMANAKA, YUTAKA KUBOKAWA,
AND MASAHARU KOMIYAMA*

Department of Applied Chemistry, University of Osaka Prefecture, Sakai, Osaka 591, Japan; and

**Department of Chemical Engineering, Faculty of Engineering, Tohoku University,
Aramaki, Aoba, Sendai 980, Japan*

Received June 23, 1987; revised September 30, 1987

Two series of Sb-Sn oxide catalysts having different Sb content and different particle sizes of SnO₂ were prepared and their propene oxidation activities were examined. Sb oxide in these Sb-Sn oxide catalysts was noncrystalline in the Sb content range of 5 to 50 at%. The concentration of Sb ions dissolved into SnO₂ lattice was estimated to be lower than 10% from the change of IR transmissions. Laser Raman and Auger electron spectroscopic analyses suggested that part of the Sb oxide is present as noncrystalline Sb(III) and Sb(V) oxides dispersed on SnO₂, whose proportion depends on the particle size of SnO₂. In the propene oxidation, the initial rates of acrylaldehyde formation increased with the increase in surface Sb content and passed through maxima at certain compositions. For both series of catalysts, the high rates and high acrylaldehyde selectivities were obtained at around the surface ratio of Sb/Sn = $\frac{1}{2}$ - $\frac{1}{3}$. A bifunctional mechanism in propene oxidation over these catalysts is discussed. The differences between SnO₂ and TiO₂ in their role as a support are also discussed. © 1988 Academic Press, Inc.

INTRODUCTION

Sb-Sn oxide is an active catalyst for the partial oxidation and the ammoxidation of olefins (1). Some workers attributed its activity for the partial oxidation to the formation of solid solution between Sb ions and SnO₂ (2-5). However, it was reported that the rate of acrylaldehyde formation in propene oxidation does not run parallel with the amount of Sb ions dissolved into SnO₂ (6). Furthermore, the solubility of Sb ions into rutile-type SnO₂ has been reported to be limited to less than a few percent (7-10). These ICI workers have proposed that complete equilibration in an Sb-Sn-O system is difficult to achieve and that at low calcination temperatures a highly disordered material provides a suitable structural environment for oxidation reactions (10). Recently, other workers have found the presence of an amorphous phase by

high-resolution electron microscopy (11). Other workers have reported that specific Sb-Sn arrangements at the surface layer of SnO₂ in which Sb ions are dissolved and the surface Sb³⁺-Sb⁵⁺ couples should be responsible for partial oxidation (12, 13).

Previously, we have reported that V-Sn (14) and Mo-Sn (15) oxide catalysts consist of noncrystalline (i.e., amorphous) V and Mo oxide due to interaction of these oxides with tin oxide. These amorphous materials have been found to have a high activity for propene oxidation and have been characterized as polymolybdates or polyvanadates. This was also the case for Mo or V oxide highly dispersed on TiO₂ (16, 17), ZrO₂ (18), and SiO₂ (19).

Along this line, the present work examines Sb-Sn oxide and Sb-Ti oxide catalysts. Their structures have been investigated by means of XRD, IR, laser Raman, and Auger electron spectroscopies. Propene oxidation and its kinetics were also studied. The relation between the surface

¹ To whom correspondence should be addressed.

TABLE I
Properties of the Catalysts Examined

Catalyst (Sb at.%)	Phase identified by XRD	Specific BET surface area (m ² g ⁻¹)
Series A		
SnO ₂	Rutile	48
Sb(10)-Sn	SnO ₂	56
Sb(20)-Sn	SnO ₂	69
Sb(30)-Sn	SnO ₂	83
Sb(40)-Sn	SnO ₂	118
Sb(50)-Sn	SnO ₂	123
Series B		
SnO ₂	Rutile	7
Sb(5)-Sn	SnO ₂	12
Sb(10)-Sn	SnO ₂	24
Sb(30)-Sn	SnO ₂	21
Sb(50)-Sn	SnO ₂	62
Sb(75)-Sn	SnO ₂ , Sb ₆ O ₁₃	44
Sb(100)	Sb ₆ O ₁₃	28
TiO ₂	Anatase (70%) + rutile (30%)	40
Sb(5.5)-Ti	TiO ₂	35
Sb(18)-Ti	TiO ₂ , Sb ₆ O ₁₃	33
Sb(55)-Ti	TiO ₂ , Sb ₆ O ₁₃	35

phases and the catalytic activities is discussed.

EXPERIMENTAL

Catalyst preparation. Two series of Sb-Sn oxide catalysts were prepared. Series A catalysts were prepared by coprecipitation from aqueous solution of SnCl₄ (Kishida Co.) and SbCl₅ (Kishida Co.) with an ammonia solution. The precipitates were dried and heated at 723 K. Series B catalysts were prepared from SnCl₂ (Kishida Co.) and SbCl₅ in the same manner and the precipitates were dried and heated at 803–823 K. In this case highly exothermic oxidation of Sn²⁺ to Sn⁴⁺ occurred during the preparation. Sb₆O₁₃ (ASTM 21-51) was prepared by the precipitation from SbCl₅ aqueous solution with ammonia and calcined at 803 K. Sb-Ti oxide catalysts were prepared as follows: SbCl₅ was dissolved into aqueous slurries containing desired quantities of TiO₂ (P-25, Degussa) and precipitated with

ammonia solution. The resulting slurries containing precipitates were filtered, dried, and heated at 723 K. The atomic percent of Sb of the catalysts and their surface area determined by the BET method are shown in Table 1.

Apparatus and procedure. X-ray diffraction patterns of the catalysts were obtained on a Rigaku Denki RAD-rA diffractometer using CuK α radiation. IR spectra of the catalysts were recorded on a Hitachi G2 spectrometer. The samples were prepared by KBr pellet techniques. Laser Raman spectra were recorded on a JASCO N-1000 spectrometer using the pellets of a ca. 150-mg catalyst sample. Auger electron spectra were obtained on a PHI 545SE spectrometer.

The catalytic oxidations of propene were carried out in a closed circulation system (ca. 300 cm³). The reaction products such as acrylaldehyde, CO₂, and CO were analyzed by gas chromatography. ¹⁸O₂ (96.7%) was obtained from MSD Canada, Ltd. The ¹⁸O percentages in the reaction products were determined with a Hitachi RMU-6E mass spectrometer using the following voltage: 80 V for CO and CO₂ and 15 V for acrylaldehyde.

RESULTS AND DISCUSSION

Propene Oxidation over Sb-Sn Oxide Catalysts

Figure 1a shows the rate of propene oxidation at 673 K. The rate decreases with an increase in the antimony content for the series A catalysts. The rate is much higher over pure SnO₂ than over pure Sb₆O₁₃ by a factor of 100–500. These results are the same as those reported by Volta *et al.* (20). In the series B catalysts, the oxidation rate first increases, passes through a maximum, and then decreases with the increase in Sb content. The activity of the series B SnO₂ is lower than that of series A.

Figure 1b illustrates the product selectivities to acrylaldehyde, CO₂, and CO. For SnO₂, the acrylaldehyde selectivities are

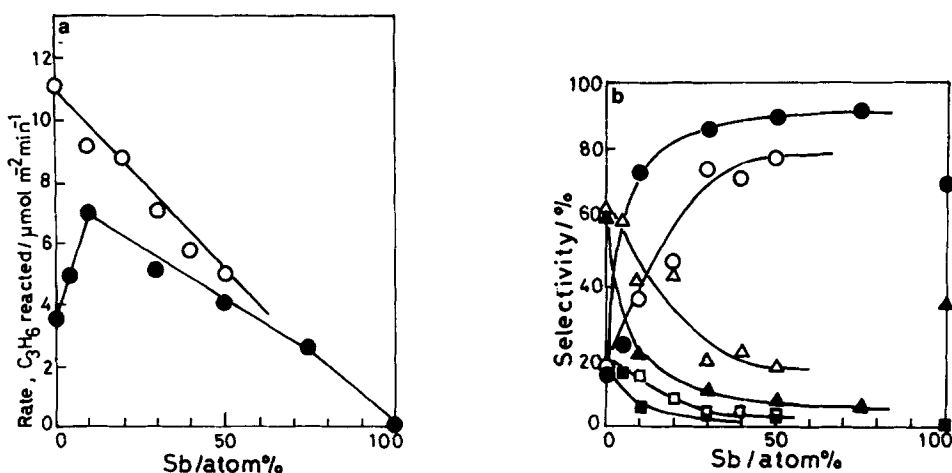


FIG. 1. (a) Rates of propene conversion on Sb-Sn oxide catalysts as a function of Sb content. (○) Series A and (●) series B. $p(\text{C}_3\text{H}_6) = 3.2$ kPa; $p(\text{O}_2) = 3.3$ kPa; temperature, 673 K. (b) Product selectivities. (○) $\text{CH}_2=\text{CHCHO}$, (□) CO, and (△) CO_2 . Empty symbols for series A and filled symbols for series B.

ca. 10%. They increase with the increase in Sb content, reaching constant values of about 80 and 90% for series A and B, respectively. Their constant value is nearly the same as that (70%) for Sb_6O_{13} catalyst. The reverse is found for CO_2 and CO formation. As shown in Fig. 2, the initial rates of acrylaldehyde formation, which were obtained at low conversion below 5%, pass through maxima in both series A and B. It is noted that the maxima are at 30 at.% Sb for series A and at 10 at.% for series B, respectively.

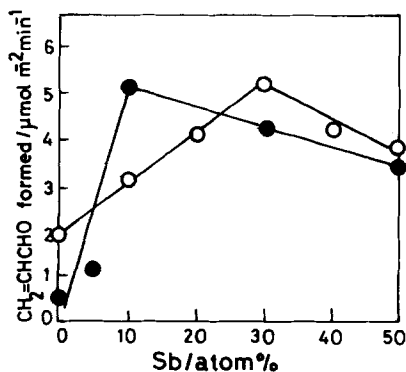


FIG. 2. Rates of acrylaldehyde formation on Sb-Sn oxide catalysts as a function of Sb content. (○) Series A and (●) series B.

As found in Figs. 1a and 1b, the oxidation activities change only twofold in the Sb content range of 5 to 30 at.% but the selectivities toward acrylaldehyde increase almost sixfold in both series A and B. Apparently, the addition of Sb enhances the acrylaldehyde formation in propene oxidation while keeping the high oxidation activity of SnO_2 itself.

Kinetics and ¹⁸O Tracer Studies of Propene Oxidation over Sb-Sn Oxides

Table 2 lists the reaction orders and the rate constants for the propene oxidation

TABLE 2
Reaction Orders and Rate Constants in Propene Oxidation over Sb-Sn Oxide Catalysts at 673 K

Catalyst (Sb at.%)	Reaction orders		Rate constants		
	C_3H_6	O_2	k_1^a	k_2^b	k_2/k_1
$\text{SnO}_2(\text{A,B})$	0	0.4-0.5	$\gg k_2$	3-8	0
$\text{Sb}(10)\text{-Sn(A)}$	0.1	0.4-0.5	160	5.5	0.03
$\text{Sb}(50)\text{-Sn(A)}$	0.3	0.4	6.3	3.7	0.6
$\text{Sb}(10)\text{-Sn(B)}$	0.3	0.5	7.7	5	0.65
Sb_6O_{13}	1	0	0.004	0.1	25

^{a,b} Calculated from the equation $R = k_1 k_2 p(\text{C}_3\text{H}_6) p(\text{O}_2)^{1/2} / (k_1 p(\text{C}_3\text{H}_6) + k_2 p(\text{O}_2)^{1/2})$; for R see Fig. 1a. Pressure ranges: $p(\text{C}_3\text{H}_6) = 0.8\text{-}8$ kPa and $p(\text{O}_2) = 0.8\text{-}8$ kPa.

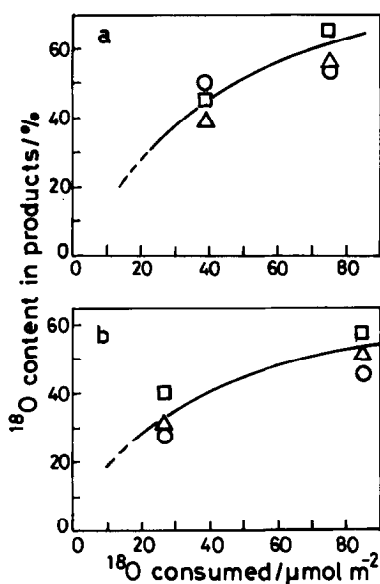


FIG. 3. ^{18}O contents in the products as a function of the amount of ^{18}O consumed during propene oxidation. $p(\text{C}_3\text{H}_6) = 3.3$ kPa; $p(^{18}\text{O}_2) = 1.1$ kPa; temperature, 673 K. (a) Sb(10)-Sn of series A; (b) Sb(10)-Sn of series B. (○) $\text{CH}_2=\text{CHCHO}$, (□) CO, and (△) CO_2 .

over Sb-Sn oxide catalysts. The propene oxidation at 673 K is zero order in C_3H_6 and 0.4–0.5 in O_2 over SnO_2 . On the other hand, it is first order in C_3H_6 and zero order in O_2 over Sb_6O_{13} . With Sb-Sn oxide catalyst, reaction orders range from 0.1 to 0.3 in C_3H_6 and 0.4 to 0.5 in O_2 with increasing Sb content. It is noted that these reaction orders change with Sb content in the case of Sb-Sn oxide catalysts.

In order to obtain information on what oxygen species are responsible for the oxidation reaction, propene oxidation was carried out using $^{18}\text{O}_2$ tracer (97 at.%). As shown in Fig. 3, ^{18}O at.% in acrylaldehyde, CO_2 , and CO are about 15–20% at initial stages over Sb(10)-Sn catalyst in both series A and B catalysts. This indicates that at initial stages ^{16}O present on or in the catalyst, i.e., lattice oxygen of Sb-Sn oxide, participates in the propene oxidation. This conclusion is consistent with those made by Christie *et al.* (21) and Pendleton *et al.* (22). Following Keulks and Krenzke (23), the extent of lattice oxygen participation

has been determined to be ca. three to four layers for Sb(10)-Sn in both series A and B, assuming uniform distribution of the incorporated ^{18}O among the sublayers of the oxides and number of oxygen atoms in unit area (ca. $20 \mu\text{mol}/\text{m}^2$). It was found that for SnO_2 only one to two layers have participated. These results suggest that oxidation reactions proceed on very thin surface sublayers of Sb-Sn oxide catalysts.

By applying a redox mechanism (17) the rate constants for the reduction step (k_1) and the reoxidation step (k_2) were calculated as shown in Table 2. With SnO_2 , the reoxidation step is rate determining. On the other hand, with Sb_6O_{13} , the reduction step is rate determining. With Sb(50)-Sn in series A and Sb(10)-Sn in series B, k_2/k_1 are 0.6 and 0.65, respectively, indicating that both step rates are nearly the same. The k_1 values with Sb(50)-Sn(A) and Sb(10)-Sn(B) are remarkably larger than those with Sb_6O_{13} by a factor of ca. 1000.

Structural Studies of Sb-Sn Oxide Catalysts

IR, laser Raman and XRD studies. X-ray diffraction patterns of these catalysts showed only the lines due to rutile-type SnO_2 in the range from 0 to 50 at.% of Sb. No lines due to Sb oxides was observed. Figure 4 shows the average particle size of

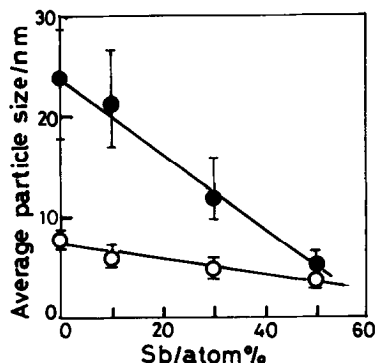


FIG. 4. Average particle sizes of SnO_2 as a function of Sb content. (○) Series A and (●) series B. The sizes are estimated using (110), (101), and (211) diffraction lines.

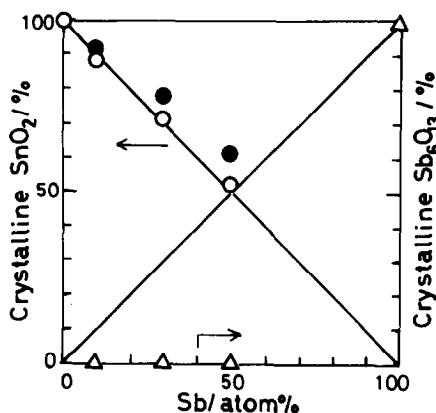


FIG. 5. Fraction of crystalline SnO_2 and Sb_6O_{13} in the Sb-Sn oxide catalysts for series A. (○) Fractions calculated from intensities of SnO_2 diluted with TiO_2 , (●) fractions of SnO_2 in the catalysts, and (△) fractions of Sb_6O_{13} .

SnO_2 calculated from the XRD line broadening (24) of (110), (101), and (211) diffractions. The sizes decrease with the increase in Sb content for both series A and B. The SnO_2 crystallite sizes in series B catalysts are several times bigger than those in series A catalysts. This difference is probably due to the difference in the starting material. Series B catalyst preparation accompanied the exothermic reaction of Sn component ($\text{Sn}^{2+} \rightarrow \text{Sn}^{4+}$) which probably enhances the SnO_2 crystallite growth.

The amount of crystalline SnO_2 in the catalysts was estimated by comparing the X-ray intensities of SnO_2 between those in the finely ground mixtures of SnO_2 and TiO_2 (P-25) and the catalysts. Since the XRD peaks of SnO_2 in the catalysts exhibited line broadening, the intensities were calculated using their peak areas. As shown in Fig. 5, the amounts of crystalline SnO_2 nearly fall on the 45° line, indicating that most of the tin oxide in the catalysts crystallizes as rutile-type SnO_2 . On the other hand, no diffraction intensities due to Sb_6O_{13} , Sb_2O_4 , and other Sb oxides were found in a range of 5 to 50 at.% Sb for both series A and B. Thus, antimony oxide is completely noncrystalline, i.e., amorphous, in this Sb content range. The pure

Sb sample exhibits the sharp and strong XRD lines due to Sb_6O_{13} . These facts indicate that the presence of Sn ions suppresses the crystallization of Sb oxide in the catalysts. As shown in Table 1, the surface area of series A catalyst increases with increasing Sb content. This seems to be caused by the presence of amorphous Sb oxide particles in addition to crystalline SnO_2 particles.

IR spectra of SnO_2 showed a broad band at 620 cm^{-1} as shown in Fig. 6. For series A catalysts in the Sb content range between 5 and 30 at.%, IR transmissions remarkably decrease and the bands due to SnO_2 completely disappear. Such a decrease in IR transmission at low Sb content seems to be due to the free electrons in the conduction bands produced by dissolution of Sb^{5+} into SnO_2 lattice (25). However, the IR transmissions are restored when more than 10 at.% of Sb is added. Such recovery of transmission indicates the decrease in the electron concentration in the conduction band. Herrmann *et al.* (6) and Volta *et al.* (13) have reported that the *n*-type semiconductivity, i.e., the concentration of electrons in the conduction band, passes through a maximum at around several percent Sb. A similar feature was also obtained in series B catalysts except that the absorp-

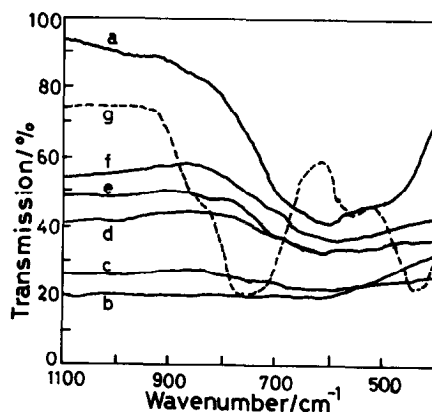


FIG. 6. IR spectra of series A Sb-Sn oxide catalysts; 2 wt% in KBr. (a) SnO_2 , (b) Sb(10)-Sn, (c) Sb(20)-Sn, (d) Sb(30)-Sn, (e) Sb(40)-Sn, (f) Sb(50)-Sn, and (g) Sb_6O_{13} .

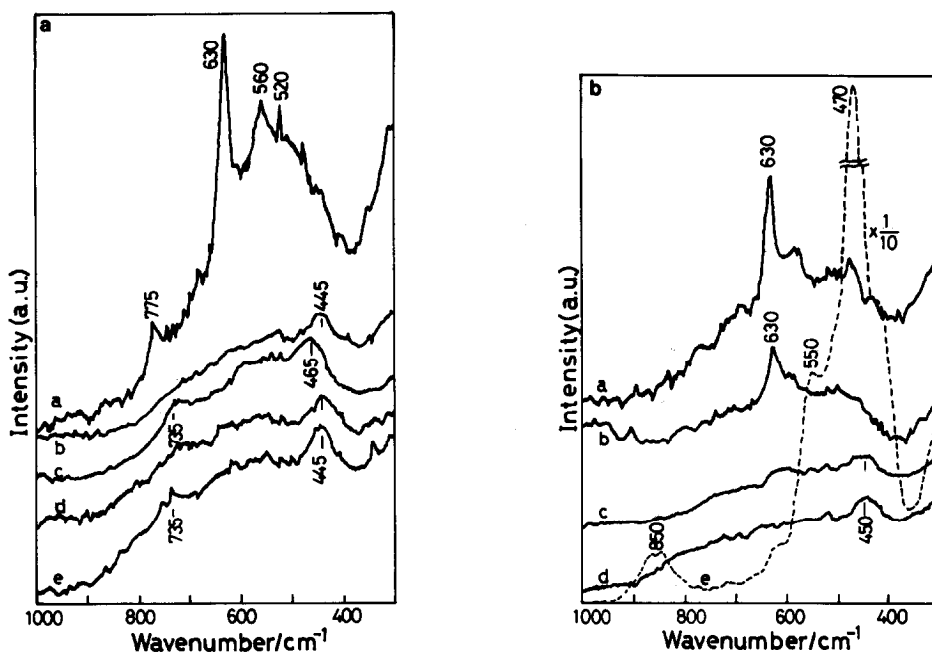


FIG. 7. (a) Laser Raman spectra of Sb-Sn oxide catalysts in series A. Ar⁺, 514.5 nm, 200 mW. (a) SnO₂, (b) Sb(10)-Sn, (c) Sb(30)-Sn, (d) Sb(40)-Sn, and (e) Sb(50)-Sn. (b) Laser Raman spectra of Sb-Sn oxide catalysts in series B. (a) SnO₂, (b) Sb(5)-Sn, (c) Sb(10)-Sn, (d) Sb(50)-Sn, and (e) Sb₆O₁₃.

tion band due to SnO₂ does not disappear completely at 5–10% Sb. The IR bands due to Sb₆O₁₃ are at 880, 780, 555, and 440 cm⁻¹ as shown in Fig. 6. With Sb-Sn oxide catalysts above 40 at.% of Sb new broad bands appear at around 600–700 cm⁻¹. These may be attributed to the amorphous Sb oxide as well as SnO₂ in the bulk phase.

The laser Raman spectra shown in Figs. 7a and 7b indicate that the bands due to SnO₂ (775, 630, 475 cm⁻¹) (26) disappear in the Sb content range of 5 to 10 at.% in both series A and B catalysts. In addition, very weak and broad bands appear at around 450 to 750 cm⁻¹. As shown in Fig. 7b(e), Sb₆O₁₃ exhibits sharp and strong bands at 420, 470, 550, and 850 cm⁻¹. The IR and Raman bands of Sb₂O₃ have been reported to appear at 410, 470, and 610 cm⁻¹ (27) and those of Sb₂O₅ at 422, 510, 590, and 817 cm⁻¹ (28). Furthermore, the IR bands of Sb₂O₄ are located at 425–440, 510, 610, 650, and 740–760 cm⁻¹ (13). Thus, the Raman bands of Sb-Sn oxide catalysts found in the

present work are not attributable to any of these oxides, viz. Sb₂O₃, Sb₆O₁₃, Sb₂O₄, and Sb₂O₅. The peaks found in the range of 450 to 750 cm⁻¹ may be the overlaps of some bands of amorphous phases on the SnO₂ surface. The IR results described above suggest that the Sb ions are present in the SnO₂ lattice as a solid solution and that its concentration is limited to below 10 at.% of Sb. Figueras *et al.* (7) and ICI workers (9, 10) have concluded that the solubility of Sb ions into SnO₂ is limited to less than a few percent. Our X-ray diffraction work suggests that amorphous Sb oxide phases are formed in the Sb content range of 5 to 50 at.% Sb. At low Sb content in the range of 10 to 30 at.%, such noncrystallinity seems to arise from the high dispersion of Sb oxide on SnO₂ surface as well as from the formation of solid solution in the moiety.

Raman spectra of crystalline compounds generally show very high and sharp bands as reported in other oxide systems (29, 30). The lack of sharp Raman bands in the

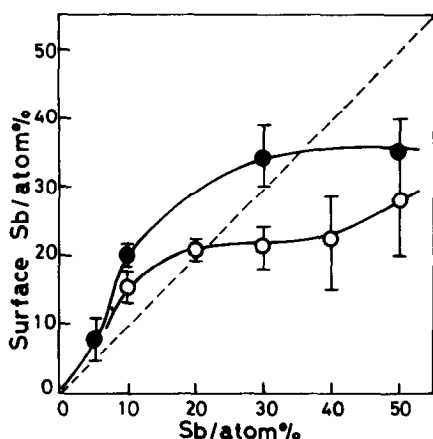


FIG. 8. Surface Sb contents determined by Auger spectroscopy. (○) Series A and (●) series B. Three kiloelectron volts of primary electron energy.

present case indicates the absence of crystalline compounds such as Sb oxides, Sb-O-Sn oxides, and SnO₂ on the catalyst surface. The lesser crystallinity of Sb oxide and Sn oxide at the surface seems to be due to some form of interaction between Sb and Sn ions. Recently, it has been reported that by using Mössbauer spectroscopy the interaction between Fe and Sn ions suppresses the crystallization of Fe oxide to Fe₂O₃ although no formation of a Sn-Fe-O compound occurs (31).

Auger electron spectroscopy. The energetic positions of Auger peaks at 425 eV ($M_5N_{4,5}N_{4,5}$) for Sn and 451 eV ($M_5N_{4,5}N_{4,5}$) for Sb scarcely changed with Sb content in the Sb content range of 10 to 50 at.% for series A catalysts. The kinetic energies of the Sb MNN peaks in these catalysts were ca. 1 eV higher than that of Sb₆O₁₃, while those of Sn ions in the catalysts were the same as that of SnO₂. These suggest that the states of Sb ions in the catalysts are different from that of Sb₆O₁₃, i.e., their Sb³⁺/Sb⁵⁺ ratios may be larger than that in Sb₆O₁₃. Berry (8) has reported the presence of both Sb³⁺ and Sb⁵⁺ by Mössbauer spectroscopy in the same Sb-Sn oxide catalysts as those prepared in this work. The surface concentrations of Sb ions were estimated using the peak-to-peak amplitude of 425-

and 451-eV peaks. As shown in Fig. 8, in the Sb content range of 10–20 at.%, the surface compositions of Sb are higher than those of bulk phase in both series A and B catalysts. Furthermore, the surface concentration of Sb increases with the increase in Sb loading and becomes constant at around 25% Sb for series A catalysts and 35% for series B. Similar results obtained by XPS have been reported by Yamazoe *et al.* (32), in which the constant value of surface Sb concentration at ca. 40–50% is reached in the Sb content range of 20 to 50%. The Sb surface concentrations for series B catalysts are higher than those for series A. The reason for these higher Sb surface concentrations in series B catalysts seems to lie in the larger SnO₂ particle sizes in these catalysts compared to those of series A catalysts: the larger the SnO₂ particle size the smaller the surface area of SnO₂, and thus the higher the surface Sb concentration for the same Sb content.

Oxidation Activities and Structures of Sb-Sn Oxide Catalysts

As shown in Fig. 2, the initial rates of acrylaldehyde formation increased with increasing Sb content for both series A and B catalysts and then passed through maxima at around 10 and 30 at.%, respectively. Simultaneously, the selectivities to acrylaldehyde become constant at around 75–80% for series A and 80–90% for series B. It is noted that the changes in the acrylaldehyde selectivities (Fig. 1b) run parallel with the changes of surface Sb concentration (Fig. 8) in both series A and B catalysts. At 10–30 at.% of Sb, the higher selectivity to acrylaldehyde formation in series B seems to be due to the higher surface concentration of Sb, which is attributed to the larger particle sizes of SnO₂ in series B as described above. The acrylaldehyde selectivity of Sb₆O₁₃ catalyst is ca. 70% which is nearly the same as those with the Sb-Sn oxide catalysts that exhibit high acrylaldehyde selectivities. These facts indicate that the ac-

rylaldehyde formation activities come from the presence of Sb ions in the catalysts.

XRD and laser Raman results indicate that while Sn oxide in the bulk is mostly crystalline SnO₂ on which Sb oxide is dispersed, the surface phase characteristics of crystalline SnO₂ as well as those of crystalline Sb₆O₁₃ are absent. Auger results also show that the surface composition which exhibits the high selectivity to acrylaldehyde ranges from Sb/Sn = $\frac{1}{4}$ to $\frac{1}{2}$ for series B and $\frac{1}{3}$ for series A. This suggests that there is an appropriate surface composition of Sn and Sb ions for the high acrylaldehyde formation. ICI workers have concluded from their XPS studies that the surface composition at around Sb/Sn = $\frac{1}{3}$ is best suited to partial oxidation (9). The current work indicates that a similar surface composition is responsible for acrylaldehyde formation, while in our case it is the amorphous phase that is active for the reaction.

The formation of CO₂ and CO is dominant on SnO₂ catalysts as shown in Fig. 1, indicating that the total oxidation activity comes mainly from SnO₂ itself at low Sb content. The complete oxidation activity of the SnO₂ support is about 100–500 times larger than those of Sb₆O₁₃ (Fig. 1a) and Sb₂O₄ (20). Thus, one may postulate that the high oxidation activity arises from the presence of tin oxide itself and high acrylaldehyde selectivity from the presence of Sb oxide as described above. Kinetic features obtained using a simple redox mechanism indicate that the reoxidation step is rate determining over SnO₂ and the reduction step over Sb₆O₁₃. However, the rates of both steps approach each other in series B Sb(10)–Sn catalyst and in series A Sb(50)–Sn. Such a change of the redox behavior with these catalysts suggests that active sites for acrylaldehyde formation are composed of both Sn and Sb ions.

Grasselli *et al.* (33, 34), however, have proposed that Sb³⁺–O and Sb⁵⁺–O moieties are responsible for π -allyl formation and oxygen insertion in acrylaldehyde formation, respectively, and that the function of

SnO_x is to provide stabilization of Sb⁵⁺–O moieties. As described above, Volta *et al.* (13) have also proposed that the surface Sb³⁺–Sb⁵⁺ couples produced on SnO₂ surface should be responsible for partial oxidation. On the other hand, McAteer (35) has suggested that acidic sites (Sn⁴⁺) and basic sites (Sb³⁺) are necessary for butene oxidation. A similar model has also been proposed by Berry (8). The present data suggest that Sn oxide itself plays an important role in giving the catalysts high oxidation activity since pure Sb oxides such as Sb₆O₁₃ and Sb₂O₄ having both Sb³⁺ and Sb⁵⁺ exhibit very low activities in propene oxidation. It is likely that a bifunctional mechanism seems to be in operation, although details are still unclear.

Oxidation Activities and Structures of Sb–Ti Oxide Catalysts

In order to compare the effect of support between SnO₂ and TiO₂, the propene oxidation characteristics and the structure of Sb–Ti oxide catalysts have also been studied. As shown in Fig. 9, TiO₂ support itself has a

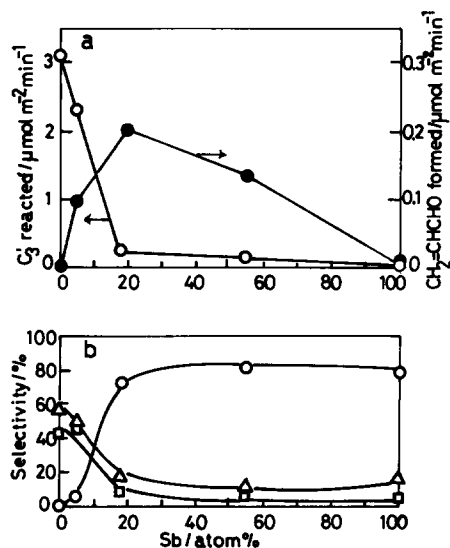


Fig. 9. (a) Rates of propene conversion over Sb–Ti oxide catalysts as a function of Sb content. $p(\text{C}_3\text{H}_6) = 3.2$ kPa; $p(\text{O}_2) = 3.3$ kPa; temperature, 673 K. (b) Product selectivities. (○) CH₂=CHCHO, (□) CO, and (△) CO₂.

considerably high activity in total oxidation of propene, while Sb(18)-Ti catalyst becomes less active by a factor of ca. 10. However, the selectivity to acrylaldehyde over this catalyst rises to 70% which is as high as that over Sb_6O_{13} catalyst. Furthermore, the catalytic activity of Sb(18)-Ti is ca. 20 times higher than that of Sb_6O_{13} . These indicate that Sb oxide is highly dispersed on TiO_2 . Similar results were reported by Zenkovets *et al.* (36) in ammoxidation reactions.

XRD patterns of Sb(5.5)-Ti oxide catalyst showed only the lines due to TiO_2 (anatase + rutile). The Sb(18) and Sb(55)-Ti catalysts showed the lines due to Sb_6O_{13} as well as TiO_2 . As has been done with the Sb-Sn oxides, the amount of crystalline Sb_6O_{13} in these catalysts was estimated by a comparison of the XRD intensities of Sb_6O_{13} between the physical mixture of Sb_6O_{13} and TiO_2 and the catalysts. The percentages of noncrystalline Sb oxide obtained were 100% for Sb(5.5)-Ti, 90% for Sb(18)-Ti, and 20% for Sb(55)-Ti.

IR spectra of these catalysts are shown in Fig. 10. With these three catalysts, very strong absorptions at around 800 cm^{-1} due to TiO_2 are observed. The bands below 800 cm^{-1} are broadly overlapped with those of TiO_2 and Sb oxide. As has been done previously (17), the absorption due to TiO_2 was subtracted from the spectra of the catalysts by placing a disk containing TiO_2 in the reference beam. With Sb(18)-Ti, the bands at around 870 and 700 cm^{-1} become visible (Fig. 10, line f). With Sb(5.5)-Ti, no bands can be observed in these ranges. With Sb(55)-Ti, the bands at 870, 760-720, and 560 cm^{-1} appear, which are attributable to those of Sb_6O_{13} (Fig. 10, line g). For Sb(18)-Ti, the spectrum resembles that of Sb_6O_{13} although the band around 760 cm^{-1} is not found in it. The laser Raman spectra of Sb(5.5)- and Sb(18)-Ti catalysts showed only the strong bands at 400, 520, and 645 cm^{-1} which are attributable to anatase-type TiO_2 . The bands of Sb oxides seemed to be masked by these bands. As shown in Fig.

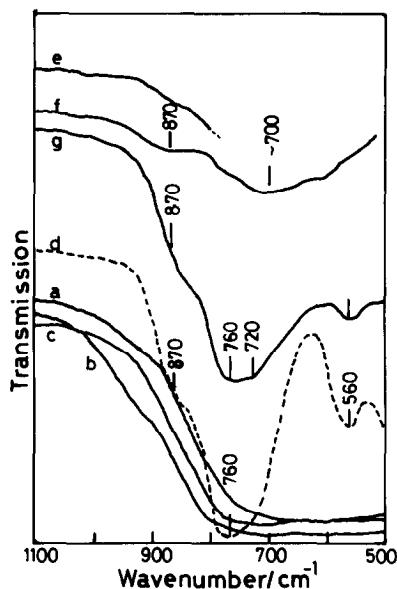


FIG. 10. IR spectra of Sb-Ti oxide catalysts; 2 wt% in KBr. (a) Sb(5)-Ti, (b) Sb(18)-Ti, (c) Sb(55)-Ti, (d) Sb_6O_{13} , (e) Sb(5)-Ti, (f) Sb(18)-Ti, and (g) Sb(55)-Ti. (e,f,g) Spectra from which the absorption due to TiO_2 was subtracted.

10, the IR transmission, i.e., background, does not decrease by the addition of Sb oxide above 1100 cm^{-1} , indicating the absence of free electrons. This suggests that Sb ions do not solute into the TiO_2 lattice at the calcination temperature (723 K). As far as XRD and IR results are concerned, amorphous Sb oxide seems to be present on the surface of TiO_2 and to have a structure similar to that of Sb_6O_{13} . Thus, in the case of TiO_2 , its high total oxidation activity disappears by the Sb oxide covering its surface. This suggests that active sites for propene oxidation are composed of only Sb oxide for the catalysts above 18 at.% Sb. Such behavior of TiO_2 support is very different from that of SnO_2 as described above; i.e., Ti ions do not take part in active sites in propene oxidation.

REFERENCES

1. Berry, F. J., in "Advances in Catalysts," Vol 30, p. 97. Academic Press, New York, 1981; Centi G., and Trifiro F., *Catal. Rev.* **28**, 165 (1986).
2. Wakabayashi K., Kamiya Y., and Ohta N., *Bull. Chem. Soc. Japan* **40**, 2172 (1967); **41**, 2776 (1968).

3. Godin, G. W., McCain, C. C., and Porter, E. A., in "Proceedings, 4th International Congress on Catalysis, Moscow, 1968" (B. A. Kazansky, Ed.), Vol. 1, p. 271. Akad. Kiado, Budapest, 1971.
4. Crozat, M., and Germain, J. E., *Bull. Soc. Chim. France* **67**, 2982 (1971).
5. Kusutova, G. N., Tarasova, D. V., Olenkova, I. P., and Chumashenko, N. N., *Kinet. Catal.* **17**, 649 (1976); **18**, 1114 (1976).
6. Herrmann, J. M. J., Fortefaix, J. L., Forissier, M., Figueras, F., and Pichat, P., *J. Chem. Soc. Faraday Trans. 1* **75**, 1346 (1979).
7. Figueras, F., Friedt, J. M., Sanchez, J. P., and Theobald, F., *J. Chem. Soc. Faraday Trans. 1* **76**, 1652 (1980).
8. Berry, F. J., *J. Catal.* **73**, 349 (1982).
9. Cross, Y. M., and Pyke, D. R., *J. Catal.* **58**, 61 (1979); Herniman, H. J., Pyke, D. R., and Reid, R., *J. Catal.* **58**, 68 (1979).
10. Pyke, D. R., Reid, R., and Tilly, R. J. D., *J. Chem. Soc. Faraday Trans. 1* **76**, 1174 (1980).
11. Berry, F. J., and Smith, D. J., *J. Catal.* **88**, 107 (1984).
12. Volta, J. C., Benaichouba, B., Mutin, I., and Vedrine, J. C., *Appl. Catal.* **8**, 215 (1983).
13. Volta, J. C., Bussiere, P., Coudurier, G., Herrmann, J. M., and Vedrine, J. C., *Appl. Catal.* **16**, 315 (1985).
14. Ono, T., Nakagawa, Y., and Kubokawa, Y., *Bull. Chem. Soc. Japan* **54**, 343 (1981).
15. Ono, T., Ikehata, T., and Kubokawa, Y., *Bull. Chem. Soc. Japan* **56**, 1284 (1983).
16. Nakagawa, Y., Ono, T., Miyata, H., and Kubokawa, Y., *J. Chem. Soc. Faraday Trans. 1* **79**, 2929 (1983).
17. Ono, T., Nakagawa, Y., Miyata, H., and Kubokawa, Y., *Bull. Chem. Soc. Japan* **57**, 1205 (1984).
18. Ono, T., Miyata, H., and Kubokawa, Y., *J. Chem. Soc. Faraday Trans. 1* **83**, 1761 (1987).
19. Ono, T., Anpo, M., and Kubokawa, Y., *J. Phys. Chem.* **90**, 4780 (1986).
20. Volta, J. C., Coudurier, G., Mutin, I., and Vedrine, J. C., *J. Chem. Soc. Chem. Commun.*, 1044 (1982).
21. Christie, J. R., Taylor, D., and McCain, C. C., *J. Chem. Soc. Faraday Trans. 1* **72**, 334 (1976).
22. Pendleton, P., and Taylor, D., *J. Chem. Soc. Faraday Trans. 1* **72**, 1114 (1976).
23. Keulks, G. W., and Krenzke, L. D., in "Proceedings, 6th International Congress on Catalysis, London, 1976" (G. C. Bond, P. B. Wells, and F. C. Tomkins, Eds.), Vol. 2, p. 806. The Chemical Society, London, 1976; Krenzke, L. D., and Keulks, G. W., *J. Catal.* **61**, 316 (1980).
24. e.g., Nitta, I., "X-sen Kesshou-Gaku (Japanese)," Vol. 1. Maruzen, Tokyo 1961.
25. e.g., Chung, J. S., and Bennett, C. O., *J. Chem. Soc. Faraday Trans. 1* **82**, 2155 (1986).
26. Scott, J. F., *J. Chem. Phys.* **53**, 852 (1970).
27. Miller, P. J., and Cody, C. A., *Spectrochim. Acta A* **38**, 555 (1982).
28. Jansen, Von M., Pebler, J., and Dehnicke, K., *Z. Anorg. Allg. Chem.* **495**, 120 (1982).
29. Chan, S. S., Wachs, I. E., and Murrell, L. L., *J. Catal.* **90**, 150 (1984).
30. Roozeboom, F., Medema, J., and Gellings, P. J., *Z. Phys. Chem. (N.F.)* **111**, 215 (1978).
31. Nakatani, Y., Sakai, M., and Matuoka, M., *Kagaku-no-Ryoiki* **37**, 102 (1983). [Japanese]
32. Yamazoe, N., Tokushige, S., Kutose, Y., and Seiyama, T., *Nippon Kagaku Kaishi*, 1885 (1982).
33. Grasselli, R. K., Brazdil, J. F., and Burrington, J. D., "Proceedings, 8th International Congress on Catalysis, Berlin, 1984," Vol. V, p. 369. Dechema, Frankfurt-am-Main, 1984.
34. Teller, R. G., Brazdil, J. F., and Grasselli, R. K., *J. Chem. Soc. Faraday Trans. 1* **81**, 1693 (1985).
35. McAteer, J. C., *J. Chem. Soc. Faraday Trans. 1* **75**, 2768 (1979).
36. Zenkovets, G. A., Tarasova, D. V., Andrushkevich, T. V., Aleshina, G. I., Nikoro, T. A., and Ravirov, R. G., *Kinet. Catal.* **20**, 307 (1979).